*Clinical Investigation*

# Left Ventricular Noncompaction Detected by Cardiac Magnetic Resonance Screening:

## A Reexamination of Diagnostic Criteria

**Anthony H. Masso, PhD**
**Carlo Uribe, MD**
**James T. Willerson, MD**
**Benjamin Y. Cheong, MD**
**Barry R. Davis, MD, PhD**

*In a previous cross-sectional screening study of 5,169 middle and high school students (mean age, 13.1 ± 1.78 yr) in which we estimated the prevalence of high-risk cardiovascular conditions associated with sudden cardiac death, we incidentally detected by cardiac magnetic resonance (CMR) 959 cases (18.6%) of left ventricular noncompaction (LVNC) that met the Petersen diagnostic criterion (noncompaction:compaction ratio >2.3). Short-axis CMR images were available for 511 of these cases (the Short-Axis Study Set). To determine how many of those cases were truly abnormal, we analyzed the short-axis images in terms of LV structural and functional variables and applied 3 published diagnostic criteria besides the Petersen criterion to our findings. The estimated prevalences were 17.5% based on trabeculated LV mass (Jacquier criterion), 7.4% based on trabeculated LV volume (Choi criterion), and 1.3% based on trabeculated LV mass and distribution (Grothoff criterion). Absent longitudinal clinical outcomes data or accepted diagnostic standards, our analysis of the screening data from the Short-Axis Study Set did not definitively differentiate normal from pathologic cases. However, it does suggest that many of the cases might be normal anatomic variants. It also suggests that cases marked by pathologically excessive LV trabeculation, even if asymptomatic, might involve unsustainable physiologic disadvantages that increase the risk of LV dysfunction, pathologic remodeling, arrhythmias, or mural thrombi. These disadvantages may escape detection, particularly in children developing from prepubescence through adolescence. Longitudinal follow-up of suspected LVNC cases to ascertain their natural history and clinical outcome is warranted.* ***(Tex Heart Inst J 2020;47(3):183-93)***

***Key words:*** *Cardiomyopathies/diagnosis; heart defects, congenital/diagnostic imaging; heart failure/etiology; heart ventricles/abnormalities/diagnostic imaging; isolated noncompaction of the ventricular myocardium/complications/diagnostic imaging; magnetic resonance imaging; ventricular dysfunction, left/etiology*

***From:*** *Departments of Cardiology (Drs. Cheong, Masso, Uribe, and Willerson) and Cardiovascular Radiology (Dr. Cheong), Texas Heart Institute; and Department of Biostatistics (Dr. Davis), The University of Texas School of Public Health, Houston, Texas 77030*

***Address for reprints:*** *Barry R. Davis, MD, PhD, Department of Biostatistics and Data Science, The University of Texas School of Public Health, 1200 Pressler St., W-916, Houston, TX 77030*

***E-mail:*** *barry.r.davis@uth.tmc.edu*



During development, the left ventricle (LV) of the heart contains bundles of muscle called trabeculae. Compaction of these trabeculae eventually transforms the heart muscle from spongelike to smooth and solid. Left ventricular noncompaction (LVNC), a rare congenital cardiomyopathy, results when compaction does not occur. In some cases, it may coincide with another myocardial disease (hypertrophic, dilated, or restrictive cardiomyopathy).

Left ventricular noncompaction can be diagnosed at any age but in many individuals goes undiagnosed until later in life. Its prevalence in the general population is unknown but ranges, according to various qualified estimates, from <0.3% to 1.26% in young children[1,2] and from 0.02% to 0.17% in adults.[3,4]

The Texas Heart Institute recently completed a large population-based screening study (the Screen to Prevent [S2P] Study) of 5,169 middle and high school students from across the Harris County (Houston), Texas, area to estimate the prevalence of congenital conditions associated with sudden cardiac death in the young.[5,6] Screening included cardiac magnetic resonance (CMR) imaging, a resting electrocardiogram (ECG), and a focused questionnaire.

Various CMR-based diagnostic criteria for LVNC have been proposed (Table I).[7-18] Because these criteria are based on small samples, various assumptions, and no accepted standard, their reliability remains in question. Applying the Petersen criterion[15]

Funding for the Screen to Prevent (S2P) Study was generously supplied by the Kinder Foundation, the Brown Foundation in Houston, and the Texas Heart Institute's general funds.

(noncompaction:compaction [NC:C] ratio >2.3) to CMR data from the S2P Study population identified 959 (18.6%) cases of LVNC.[5,6] This observational finding, which is at odds with published estimates of LVNC prevalence,[1-4] prompted us to examine information from the S2P Study more closely by using CMR-based metrics to determine whether the cases of LVNC detected by applying the Petersen criterion were truly abnormal or just normal anatomic variants.

## Patients and Methods

Data for the present study were obtained from the S2P Study database. The 5,169 voluntary participants in the S2P Study (mean age, 13.1 ± 1.78 yr) were a representative sample of the general population of children 11 to 18 years old in Harris County (Houston), Texas. Of the 959 participants in the S2P Study identified as having LVNC, 511 had short-axis CMR imaging results available in the database. This cohort, called the Short-Axis Study Set, was the subject of the current analyses.

Data collected in the S2P Study included demographics, vital signs, brief cardiac medical histories, CMR-based screening data, resting ECGs, and results of overall screening evaluations by cardiology experts. The CMR imaging protocol for the S2P Study, which was designed for primary screening and not full-fledged clinical imaging, included acquisition of long-axis views (2-chamber, 4-chamber, and LV outflow tract), acquisition of short-axis views (for many but not all cases), and sequences for detecting coronary artery origins and proximal courses. Sixteen-lead ECGs were acquired and

**TABLE I.** Cardiac Magnetic Resonance–Based Criteria for Diagnosis of Left Ventricular Noncompaction

| Criteria Reference | CMR View, Cardiac Cycle Phase | Criteria | Study Cohort | Sensitivity | Specificity | Basis for Criteria |
|---|---|---|---|---|---|---|
| Petersen SE, et al.[15] (2005) | Long-axis, diastole | Maximal NC:C wall thickness ratio >2.3 | N=177<br>• 45 Healthy volunteers<br>• 25 Athletes<br>• 14 DCM<br>• 39 HCM<br>• 17 Hypertension<br>• 30 Aortic stenosis<br>• 7 LVNC (clinical diagnosis) | 86% | 99% | "Pathological LVNC [as distinguished] from the [lesser] degrees of non-compaction observed in samples of healthy, dilated, and hypertrophied hearts" |
| Jacquier A, et al.[11] (2010) | Short-axis, end-diastole | Trabeculated LV mass >20% of total LV mass | N=64<br>• 16 Healthy control subjects<br>• 16 DCM<br>• 16 HCM<br>• 16 LVNC | 91.6% | 86.5% | The 16 cases of LVNC diagnosed per Jenni criteria,* the gold standard |
| Grothoff M, et al.[9] (2012) | Short-axis, end-diastole | Trabeculated LV mass >25% of total LV mass<br>Trabeculated LV mass/BSA >15 g/m$^2$<br>NC:C >3 in segments 1–3, 7–16<br>NC:C >2 in segments 4–6 | N=57<br>• 24 Healthy control subjects<br>• 10 HCM<br>• 11 DCM<br>• 12 LVNC | 75% | 100% | Retrospective assessment of the 12 cases of LVNC diagnosed per Jenni criteria,* used as the reference, and additional clinical considerations |
| Choi Y, et al.[8] (2016) | Short-axis, end-diastole | Trabeculated LV volume >35% of total LV volume | N=145<br>• 31 Healthy control subjects<br>• 24 Isolated LVNC<br>• 33 Nonisolated LVNC<br>• 30 DCM with noncompaction<br>• 27 DCM | 66.1% | 89.7% | The 33 cases of nonisolated LVNC diagnosed per Jenni criteria,* which were used as the reference for assessing sensitivity and specificity of the proposed trabeculated LV volume criterion |

BSA = body surface area; CMR = cardiac magnetic resonance; DCM = dilated cardiomyopathy; HCM = hypertrophic cardiomyopathy; LV = left ventricular; LVNC = left ventricular noncompaction; NC:C = noncompaction:compaction

*As proposed by Jenni and associates,[18] echocardiography-based criteria for LVNC in the absence of other cardiac anomalies include a 2-layer LV myocardial structure with a thin, compacted outer band and a much thicker, noncompacted inner layer of trabecular meshwork with deep endocardial spaces; a maximum end-systolic NC:C ratio >2; and color Doppler evidence of deeply perfused intertrabecular recesses.

reviewed by an experienced electrophysiologist. These data were acquired, evaluated, deidentified, and used as provided for in the institutional review board–approved protocol for the S2P Study.[5,6]

### Short-Axis Image Measurements

The current analysis relied on the use of long- and short-axis CMR images acquired in the S2P Study. Long-axis CMR imaging enables rapid detection of a distinct layer of excessive ventricular trabeculation. Short-axis imaging permits more accurate delineation of the compact LV myocardial layer and the contained ventricular cavity; when present, the additional layer of ventricular trabeculae can also be distinguished from the compact layer. Of note, however, measurements derived from both long- and short-axis images are subject to bias and error due to imaging plane location and orientation; in addition, nonperpendicularity relative to the long axis of short-axis images may introduce systematic errors that might be accentuated in the apical region.

Although current imaging technology does not enable full resolution of the complexities of ventricular trabeculae, the trained observer can distinguish gross features, including the location, local apparent thickness, and distinctive layering of trabeculae against the compact myocardial walls and their irregular boundary with the ventricular cavity. Therefore, the conventional tools and methods for quantifying imaging-derived myocardial variables in the normal heart were used to evaluate LV trabeculation, especially the volume of the trabeculated region.

The short-axis imaging stacks used for screening in the S2P Study typically included 8 slices, each 8 mm thick and separated by 1 mm. The slices were acquired from just below the mitral valve to near the apex. Additional technical details of the CMR imaging procedure are available elsewhere.[5,6]

Clear and consistent short-axis images of the LV cavity, along with clear delineations of the trabeculated layer and compact myocardium, were obtained for the Short-Axis Study Set at both end-diastole and end-systole. The epicardial and endocardial contours were drawn by 2 experienced cardiac radiologists (CU and BYC). To quantify areas of excessive trabeculation, borders were drawn between the compact myocardium and the trabeculated layer, as well as between the trabeculated layer and the open ventricular cavity (Fig. 1).

Epicardial and endocardial contours were analyzed to generate volume estimates for the LV cavity, trabeculated region, and compact myocardium according to established standards.[19] From these measurements, values for other structural and functional variables were derived. Contouring and measurement of CMR images were done with use of cvi42 image-postprocessing software (Circle Cardiovascular Imaging Inc.). Conventional image-processing software was used to generate volume and mass estimates for the various structures delineated by the contours described above and displayed in Figure 1. For example, the green and red contours were analyzed with the cvi42 software to estimate the volume and mass of the compact LV myocardium. The green and blue contours were analyzed to obtain aggregate volume estimates of compact and trabeculated (noncompact) LV myocardium. The trabeculated LV

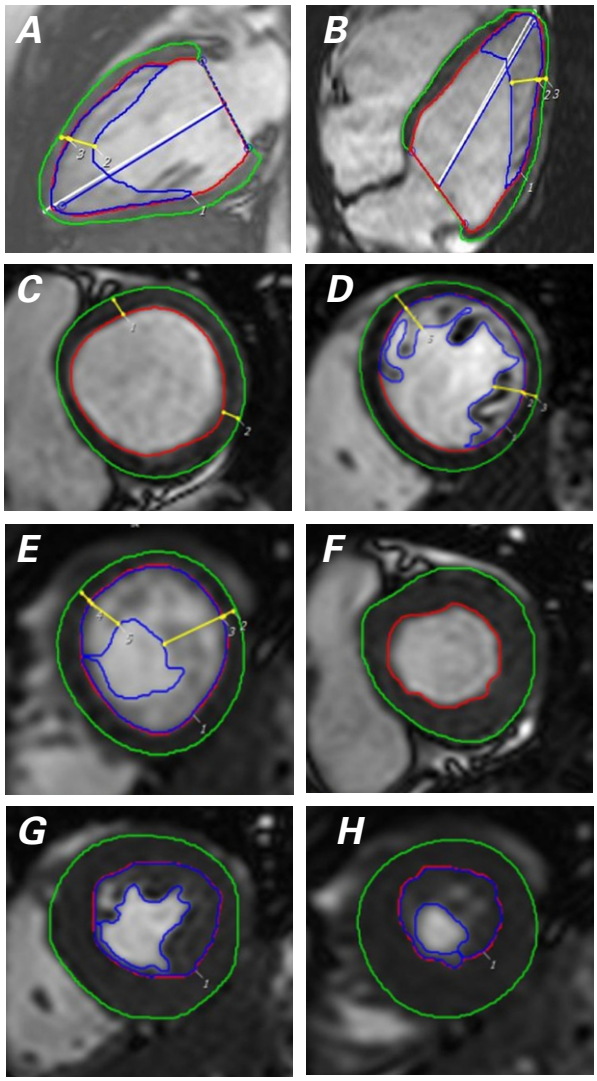


***Fig. 1*** *Representative cardiac magnetic resonance images show* ***A****) 2-chamber and* ***B****) 4-chamber views of the epicardial contour of the left ventricle, as well as the endocardial contours of the compact layer and trabeculated (noncompact) region; short-axis views of the epicardial and endocardial contours at end-diastole at* ***C****) basal,* ***D****) mid, and* ***E****) apical levels; and short-axis views of the epicardial and endocardial contours at end-systole at* ***F****) basal,* ***G****) mid, and* ***H****) apical levels. Epicardial contours are green; endocardial contours, red; trabeculated (noncompact) region contours, blue. The dotted blue line shown in the 2-chamber view in* ***A****) indicates the left ventricle's conventionally defined basal limit. The numbered yellow line segments shown in* ***A****) through* ***E****) are included to illustrate compact and trabeculated (noncompact) layer thicknesses in the different images of the left ventricle as they might be used in applying the Petersen criterion.*

volume was then obtained by difference. Last, estimates of trabeculated LV volume at end-diastole and end-systole were obtained and used to assess changes in trabeculated LV myocardium across the cardiac cycle.

### Trabeculated Left Ventricular Mapping

For each case, the short-axis images were used to map the trabeculated LV as described above and to measure its areal extent and the thicknesses of noncompact (trabeculated) and compact myocardial tissue at end-diastole. Each short-axis image slice was subdivided into 6 segments for this purpose. The fraction of all segments in which trabeculation met the Petersen criterion (NC:C ratio, >2.3) served as a proxy for the interior LV surface area covered with trabeculae meeting that criterion.

### Measurement Consistency

As a first step toward better characterizing the effects of excessive LV trabeculation, we used conventional volumetric measurements derived from short-axis LV images to generate a 2-dimensional, quantitative description of LV trabeculation in terms of the following:

- $EF_e$ = LV ejection fraction (LVEF) estimated with trabeculae and papillary muscles excluded from the blood pool;
- $V_d^T$ = volume of trabeculae at end-diastole as estimated from LV images;
- $V_s^T$ = volume of trabeculae at end-systole estimated from LV images; and
- $LVM_c$ = mass of LV compact myocardium estimated from short-axis LV images.

To ensure consistency and to avoid systematic errors, all imaging-based volumetric measurements were subjected to the following logic checks:

- The aggregate volume of LV trabeculae and compact myocardium at end-diastole was greater than at end-systole.
- The aggregate volume of LV trabeculae and compact myocardium at end-systole was greater than that of the compact myocardium alone.
- The LV cavity volume with trabeculae included in the blood pool was greater than the LV cavity volume with trabeculae excluded from the blood pool, at both end-diastole and end-systole.
- The LV stroke volume estimated from contours that included trabeculae in the blood pool was greater than the LV stroke volume estimated from contours that excluded trabeculae from the blood pool.

### Net Relative Trabeculation Mass

We used short-axis LV images to estimate more accurately the trabeculated LV mass, specifically excluding the mass of the blood contained in the intertrabecular luminal spaces. This variable was defined as the net relative trabeculation mass (NRTM).

Estimates for NRTM were derived by using the values for $EF_e$, $V_d^T$, and $V_s^T$ derived from analysis of short-axis LV images and also by defining $\phi_d^T$ as the fraction of trabeculated LV volume occupied by intertrabecular luminal spaces at end-diastole. Hence, this gave:

$$V_d^T \times \phi_d^T,$$

which describes the volume of blood contained in intertrabecular luminal spaces at end-diastole.

For intertrabecular luminal spaces open to the ventricular cavity, we assumed that the fraction of blood volume ejected at systole from those intertrabecular luminal spaces was equal to the fraction ejected from the ventricular cavity. Thus, equating the calculation of the former fraction with the separate estimate of the latter fraction enabled calculation of $\phi_d^T$ as follows:

$$\phi_d^T = [\ (V_d^T - V_s^T) / V_d^T\ ] \times [\ 1 / EF_e\ ],$$

where $0 < \phi_d^T < 1$.

The net mass of LV trabeculations ($m^T$), which excluded the mass of the blood contained in the intertrabecular luminal spaces at end-diastole, was given by the following equation:

$$m^T = V_d^T \times (1 - \phi_d^T) \times 1.05,$$

where the factor 1.05 is the assumed density (g/mL) of trabeculated tissue.

The value of NRTM, expressed as a percentage of total LV mass, was given by the following equation:

$$NRTM = 100 \times [\ m^T / (\ m^T + LVM_c\ )\ ],$$

where $LVM_c$ is the mass of LV compact myocardium estimated from short-axis LV images.

### Estimation of Left Ventricular Noncompaction Prevalence

To estimate the prevalence of LVNC, we applied the CMR-based criteria for LVNC diagnosis proposed by the Choi,[8] Jacquier,[11] and Grothoff[9] groups (Table I) to the LV volume and mass estimates that we had derived from measurements of the short-axis images for the Short-Axis Study Set.

### Statistical Analysis

Measurements of LV variables were indexed to body surface area (BSA) (computed by the Mosteller formula) where applicable. Continuous data were summarized

as mean ± SD. Statistical comparisons were performed with use of *t* tests. $P < 0.05$ was considered statistically significant. Pearson and intraclass correlation coefficient analyses and Bland-Altman analyses were performed to evaluate measurement repeatability. Stata version 14.0 software (StataCorp LLC) was used for all analyses.

## Results

The Short-Axis Study Set (N=511) was comparable to the full S2P Study cohort (N=5,169) with regard to age, race, ethnicity, and sex distribution (Table II). Ninety-four (18.4%) participants in the Short-Axis Study Set reported symptoms: shortness of breath with exercise in 60 (11.7%), chest pain in 22 (4.3%), syncope with exercise in 7 (1.4%), and syncope at rest in 5 (1%). Thirteen participants had cardiac disorders: hypertrophic cardiomyopathy in 2; dilated cardiomyopathy in 3; anomalous origin of coronary arteries in 3; and the ECG abnormalities Wolff-Parkinson-White syndrome in 2, prolonged QT interval (QTc >470 ms) in 2, and fixed ventricular bigeminy in one.

### Left Ventricular Volume Estimates

Left ventricular end-diastolic volume (LVEDV) estimates were affected by the presence of trabeculae and their inclusion in or exclusion from the blood pool. Supplemental Table I presents data from 2 sample cases to demonstrate how we derived our estimates of LV trabeculation–related variables from conventional imaging-derived volumetric measurements. Supplemental Table II presents BSA-indexed summary statistics for those variables for the entire Short-Axis Study Set.

The mean indexed LVEDV was significantly greater when trabeculae were included in the blood pool (76.9 ± 12.2 vs 49.2 ± 9.6 mL/m$^2$; $P < 0.001$) (Fig. 2). The

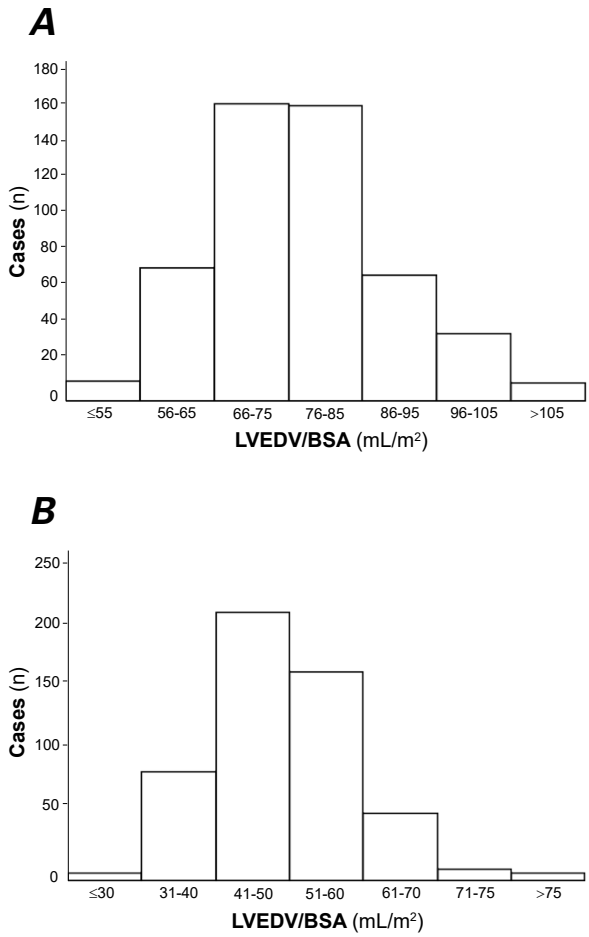


***Fig. 2*** *Graphs show the frequency of measurements of left ventricular end-diastolic volume (LVEDV) indexed to body surface area (BSA) with trabeculae* ***A****) included in the blood pool (mean, 76.9 ± 12.2 mL/m$^2$) and* ***B****) excluded from the blood pool (mean, 49.2 ± 9.6 mL/m$^2$) in the Short-Axis Study Set (N=511). The mean LVEDV was significantly greater when trabeculae were included (P <0.001).*

**TABLE II.** Demographic Characteristics of the Short-Axis Study Set

| Characteristic | Short-Axis Study Set | | | |
|---|---|---|---|---|
| | **Female** n=194 (38%) | **Male** n=317 (62%) | **Total** N=511 | **Screen to Prevent Study Set** (N=5,169)* |
| Age (yr) | 13.4 ± 1.89 | 13.3 ± 1.68 | 13.1 ± 1.63 | 13.1 ± 1.78 |
| Race/ethnicity | | | | |
| Asian | 16 (8.2) | 11 (3.5) | 27 (5.3) | 526 (10.2) |
| Black | 63 (32.5) | 99 (31.2) | 162 (31.7) | 1,185 (22.9) |
| Hispanic | 41 (21.1) | 62 (19.6) | 103 (20.2) | 980 (19.0) |
| White | 57 (29.4) | 109 (34.4) | 166 (32.5) | 1,647 (31.9) |
| Other** | 17 (8.8) | 36 (11.4) | 53 (10.4) | 831 (16.1) |

* 2,274 females (44%) and 2,895 males (56%)
** American Indian, Hawaiian, Pacific Islander, or multiracial

Data are presented as mean ± SD or as number and percentage.

trabeculated LV region had a spectrum of presentations and a measurable volume at end-diastole (mean, 25.5 ± 8.1 mL/m$^2$). The volume of blood contained in intertrabecular luminal spaces was therefore dependent on the extent and structure of the trabeculated region (Fig. 3).

The trabeculated region was apparently compressed across the cardiac cycle. The mean reduction in its volume at end-systole was 52.5% ± 17.2%, reflecting primarily compression of the intertrabecular luminal spaces (Fig. 4). Thus, blood ejected from the intertrabecular luminal spaces at end-systole necessarily became part of the total LV stroke volume, and the wide range of trabeculated region compression suggests a varied gross structure (that is, a spectrum of intertrabecular luminal space volumes).

Including papillary muscles and trabeculae in the LV blood pool resulted in the systematic underestimation of LVEF (Fig. 5).

### Measurement Repeatability

The repeatability of imaging-derived volumetric measurements was evaluated in a randomly selected sample of 28 (5.5%) cases to check the consistency of the initial contouring done as described above. In brief, repeat measurements of 7 distinct variables derived from primary volumetric estimates were generated by the image-postprocessing software from the contours as initially drawn at baseline. Baseline and repeat measurements were made approximately one year apart. As expected, and as shown by correlation and bias analyses, measurements at end-systole were more susceptible to error (Table III). These errors were propagated because LV stroke volume estimates were affected by the presence of trabeculae.

### Estimated Prevalence of Left Ventricular Noncompaction

After applying the criterion of Jacquier and associates[11] to the Short-Axis Study Set, we identified 482 cases as abnormal, a prevalence of 17.5%. In contrast, after applying the criterion of Choi and associates,[8] we identified 205 cases as abnormal, a prevalence of 7.4%. This mismatch between these 2 estimates of LVNC prevalence is shown in Figure 6. In addition, our trabeculation modeling indicated that 163 (17%) of cases in the Short-Axis Study Set met the Petersen criterion[15] but had trabeculae of no significant mass (that is, open, lace-like trabeculae that on long-axis images appeared to be very thick). Thus, relatively few of the LVNC cases in the Short-Axis Study Set that met the Petersen criterion also had high NRTM values (Fig. 7).

We also applied the CMR mass–based criteria proposed by Grothoff and associates[9] and our own method for estimating trabeculated LV mass in terms of NRTM (Fig. 8). This identified 35 (3.7%) cases in the Short-Axis Study Set as abnormal, corresponding to a prevalence of 1.3% when this finding was extrapolated to the larger S2P Study cohort.

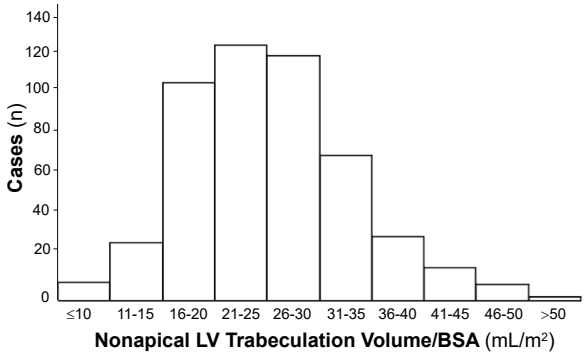


***Fig. 3*** *Graph shows the frequency of measurements of nonapical left ventricular (LV) trabeculation volume indexed to body surface area (BSA) (mean, 25.2 ± 8.1 mL/m$^2$) in the Short-Axis Study Set (N=511).*

## Discussion

Our detailed analysis of 511 CMR-detected cases of LVNC, originally identified according to the Petersen criterion,[15] suggests that many were normal anatomic variants. After we applied the criteria of Grothoff and colleagues[9] to our cohort, the estimated prevalence of LVNC was much lower than that in our original S2P Study. The Petersen criterion is too broad, but other criteria (for example, those proposed by the Grothoff,[9] Jacquier,[11] and Choi[8] groups) may be no more reliable, as we have shown in this analysis.

Left ventricular noncompaction is a poorly understood cardiomyopathy[20] with various reported phenotypes (for example, isolated or concomitant with hypertrophic or dilated cardiomyopathy) that may change over time.[21] Its cause is uncertain.[7,20,21] Multiple genetic markers have been identified, and potential

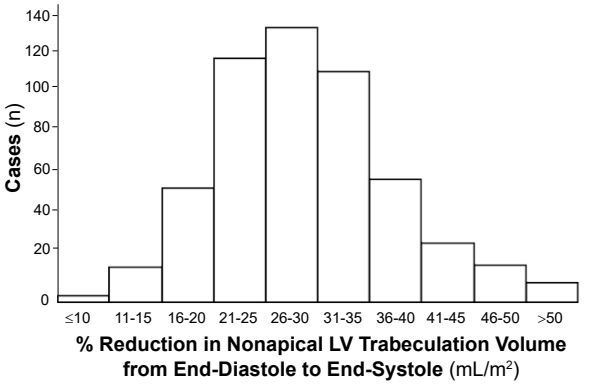


***Fig. 4*** *Graph shows the frequency of measurements of nonapical left ventricular (LV) trabeculated region compression in terms of percent reduction from end-diastole to end-systole (mean, 52.5 ± 17.2%), an indication of its contribution to LV end-systolic volume, in the Short-Axis Study Set (N=511).*

**TABLE III.** Imaging Measurement Repeatability

| Variable | Pearson Coefficient[a] | Intraclass Correlation Coefficient | Bland-Altman Analysis | | |
|---|---|---|---|---|---|
| | | | Mean Difference[b] | 95% CI[c] | Limits of Agreement |
| **Trabeculae included in blood pool** | | | | | |
| EDV | 0.927 | 0.915 | −4.68 | −9.89 to 0.52 | −31.52 to 22.15 |
| ESV | 0.867 | 0.829 | −4.88 | −8.24 to −1.53 | −22.17 to 12.40 |
| $LVM_c$ | 0.955 | 0.955 | −0.72 | −4.08 to 2.65 | −18.05 to 16.61 |
| **Trabeculae excluded from blood pool** | | | | | |
| EDV | 0.930 | 0.894 | −6.48 | −10.10 to −2.87 | −25.10 to 12.13 |
| ESV | 0.690 | 0.665 | −2.77 | −5.54 to 0.12 | −17.65 to 12.12 |
| $V_d^T$ | 0.915 | 0.917 | −1.81 | −8.16 to 4.53 | −34.52 to 30.90 |
| $V_s^T$ | 0.946 | 0.942 | −3.79 | −8.42 to 0.83 | −27.63 to 20.05 |

EDV = end-diastolic volume; ESV = end-systolic volume; LV = left ventricular; $LVM_c$ = mass of LV compact myocardium; $V_d^T$ = volume of trabeculae at end-diastole; $V_s^T$ = volume of trabeculae at end-systole

[a]Pearson and intraclass correlation coefficients are consistent and, as expected, point to a lower correlation for ESV than for other variables.

[b]With relatively broad limits of agreement (Bland-Altman), the mean difference between repeated measurements shows a statistically significant measurement bias for 2 of the 7 variables even when repeat measurements are correlated.

[c]Confidence intervals for the mean differences between repeated measurements indicate generally acceptable repeatability.

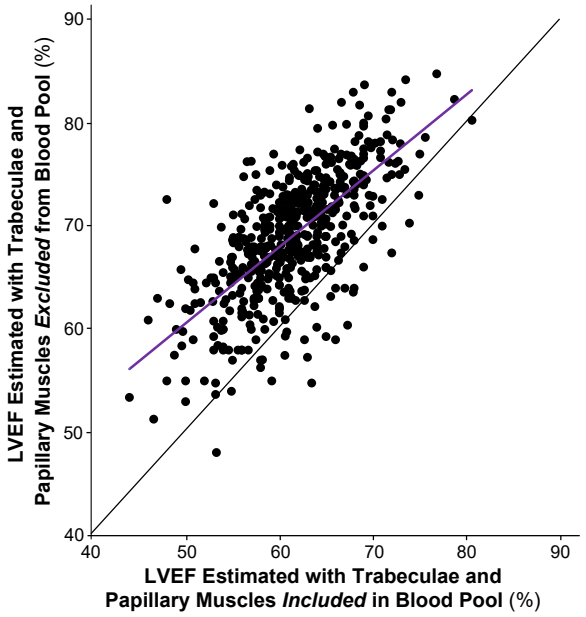


***Fig. 5*** *Scatter plot shows the distribution of left ventricular ejection fraction (LVEF) in the Short-Axis Study Set (N=511), as estimated with trabeculae and papillary muscles included in (x-axis) or excluded from (y-axis) the blood pool. The line of best fit is shown in purple; the line of identity, in black.*

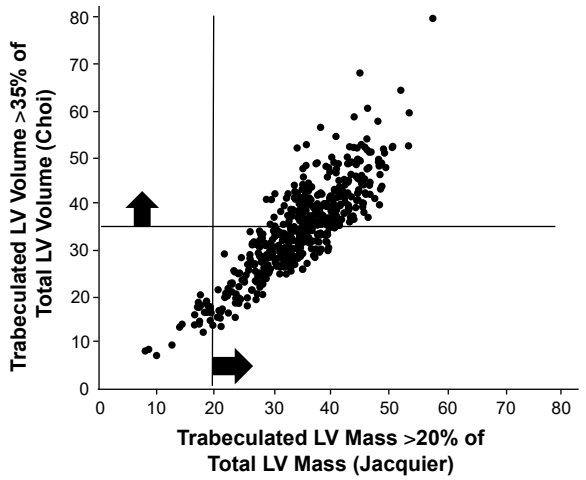


***Fig. 6*** *Scatter plot shows the distribution of cases of left ventricular noncompaction identified by applying the criteria of Choi and colleagues (trabeculated LV volume >35% of total left ventricular [LV] volume)[8] and Jacquier and associates (trabeculated LV mass >20% of total LV mass)[11] to the Short-Axis Study Set (N=511).*

familial involvement is often cited.[22-34] As annotated in the ClinVar public archive of genetic variants[35] and reported elsewhere,[22-25,27-36] more than 70 pathogenic or likely pathogenic variants in more than 20 genes have been deemed to be of clinical significance in LVNC. Not all of those genetic variants may cause disease, and mutations in several LVNC-linked genes are also linked with other cardiomyopathies.

Current diagnostic criteria for LVNC are unreliable,[7-18,23] and treatment is driven by phenotype and symptoms and aimed at preventing or treating heart failure.[37-40] There is no cure. Neonates and very young children with more severe phenotypes have poor out-

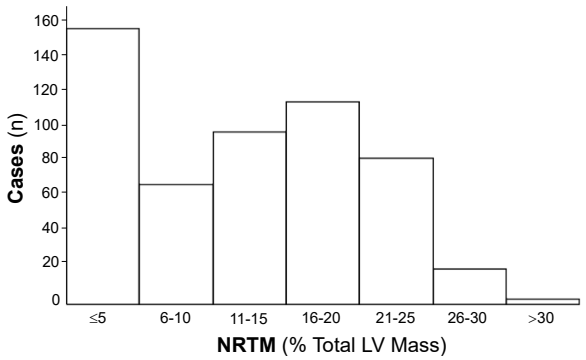


***Fig. 7*** *Graph shows the frequency of estimates of left ventricular (LV) net relative trabeculation mass (NRTM), expressed as percentage of total LV mass, in the Short-Axis Study Set (N=511). The NRTM excludes the mass of the blood contained in intertrabecular luminal spaces.*

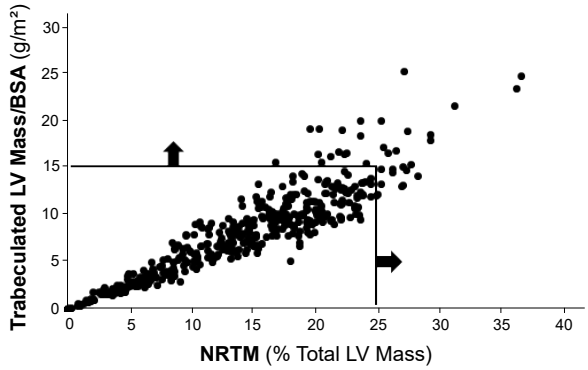


***Fig. 8*** *Scatter plot shows the distribution of cases of left ventricular noncompaction (LVNC) in the Short-Axis Study Set (N=511) identified by applying the criterion of Grothoff and colleagues[9] and our method for estimating trabeculated LV mass in terms of net relative trabeculation mass (NRTM). The estimated LVNC prevalence was 1.3% when these data were extrapolated to the original Screen to Prevent Study cohort.*

comes and low survival rates.[2,39,41] Some young people with isolated LVNC may have a better prognosis.[23,42]

It is unclear whether poor outcomes in the young are caused by LVNC, or whether LVNC is secondary to another cause of those outcomes.[43,44] Case reports repeatedly point to the clinical complexity of LVNC cases,[45-57] and numerous other studies document the limited understanding of this condition.[7,50,58,59] Asymptomatic LVNC is often identified incidentally, and its clinical management typically includes follow-up with prophylactic measures, such as anticoagulation and antiarrhythmia therapies, and restrictions on physical activity.[37-40] The effect of these restrictions on lifestyle choices for children is complex and not fully understood.[60,61] The change in some LVNC phenotypes over time is of concern for children as they develop from prepubescence to early adolescence. Evolving LVNC phenotypes require adaptive clinical surveillance and treatment strategies.[20]

## Limitations

This work was based on cross-sectional CMR-based data obtained at primary screening during the S2P Study and focused on analyzing objective measurements derived from those data. Longitudinal measurements may provide more insight. Participants in the S2P primary screening study took part voluntarily and, therefore, do not constitute a rigorous sample of the general population. That said, the demographics of the S2P Study population compare favorably with those of the general population in the greater Houston, Texas, area.[5]

In analyzing short-axis images from the 511 participants in the Short-Axis Study Set, we considered only the nonapical regions of the heart and thus may have underestimated trabeculated LV mass. We made no attempt to exclude the papillary muscles from the regional volume measurements of LV trabeculae. Although this may have introduced a systematic but limited bias into our estimates of trabeculated LV mass, we think that this bias had little effect on estimates of the volume of nonapical intertrabecular luminal spaces.

No clinical assessments were performed to confirm LVNC in study participants. In addition, we did not acquire any longitudinal follow-up data that would help to detect changes or provide information on clinical outcomes.

The cases of LVNC that we identified during screening in the S2P Study included several cardiac disorders associated with LVNC; however, confirmatory clinical evaluations and longitudinal follow-up are needed to ascertain their clinical course. One-time screening does not allow detection of changes in a cardiac disorder over time, and small sample size impedes reliable estimation of the underlying prevalence of each of those disorders.

Observer-related variability and measurement error, especially regarding the visual delineation of the irregular features of ventricular trabeculae, markedly affect the imaging-derived quantification of cardiac variables. Automated image quantification will improve measurement accuracy and precision and help provide information that could be used to reliably evaluate patients presenting with excessive trabeculation. Quantification of LV function and mass by contour drawing is widespread, and there is good understanding of measurement variability[62] and the usefulness of CMR-based measurement in defining significant changes.[63] We acknowledge that automation of CMR image analysis, although not routine, is advancing. Examples include automated endocardial border detection,[64-66] selection of short-axis slices for automated quantification,[67] LV segmentation and finite element modeling,[68,69] application of "machine learning" to contouring,[70] and fractal analysis of myocardial trabeculation.[71]

## Conclusions

Our findings suggest that many of the 511 suspected cases of LVNC identified in our previous S2P Study may have been normal anatomic variants and that many could be reclassified as normal on the basis of our current findings. The remaining cases, including those that were largely asymptomatic, may have involved subclinical changes in LV structure and function. Therefore, the true prevalence of pathologically excessive LV trabeculation in our 11- to 18-year-old cohort in the S2P Study is probably <1%, while the severity and clinical significance of potential LVNC remain unknown. Young people presenting with excessive LV trabeculation, even if asymptomatic, may exhibit distinct structural features that are physiologically disadvantageous. Whether aggravated by exertion (for example, by participation in sports) or by normal development from puberty into early adolescence, the eventual cumulative effect may be reduced ventricular function, with its associated complications and risks. Excessive LV trabeculation, even if initially asymptomatic, may serve as a substrate for malignant arrhythmias or thrombus formation. In light of our findings based on a population sample, longitudinal follow-up of individuals with suspected LVNC is warranted in general. A more detailed analysis of other CMR-based metrics in the Short-Axis Study Set will be presented in the future.

## Acknowledgments

Raja Muthupillai, PhD, provided the CMR imaging protocol and guidance regarding imaging quality control. Veronica V. Lenge De Rosen, MD, reviewed the CMR screening data to help identify potential abnormalities. Stephen N. Palmer, PhD, ELS, contributed to the editing of the manuscript.

## Supplementary Material

Supplemental tables for this article are available at 10.14503_thij-19-7157.s1.pdf.

## References

1. Gati S, Papadakis M, Papamichael ND, Zaidi A, Sheikh N, Reed M, et al. Reversible de novo left ventricular trabeculations in pregnant women: implications for the diagnosis of left ventricular noncompaction in low-risk populations. Circulation 2014;130(6):475-83.
2. Koh C, Lee PW, Yung TC, Lun KS, Cheung YF. Left ventricular noncompaction in children. Congenit Heart Dis 2009;4(4):288-94.
3. Stanton C, Bruce C, Connolly H, Brady P, Syed I, Hodge D, et al. Isolated left ventricular noncompaction syndrome. Am J Cardiol 2009;104(8):1135-8.
4. Gati S, Rajani R, Carr-White GS, Chambers JB. Adult left ventricular noncompaction: reappraisal of current diagnostic imaging modalities. JACC Cardiovasc Imaging 2014;7(12):1266-75.
5. Angelini P, Cheong BY, Lenge De Rosen VV, Lopez A, Uribe C, Masso AH, et al. High-risk cardiovascular conditions in sports-related sudden death: prevalence in 5,169 schoolchildren screened via cardiac magnetic resonance. Tex Heart Inst J 2018;45(4):205-13.
6. Angelini P, Cheong BY, Lenge De Rosen VV, Lopez JA, Uribe C, Masso AH, et al. Magnetic resonance imaging-based screening study in a general population of adolescents. J Am Coll Cardiol 2018;71(5):579-80.
7. Anderson RH, Jensen B, Mohun TJ, Petersen SE, Aung N, Zemrak F, et al. Key questions relating to left ventricular noncompaction cardiomyopathy: is the emperor still wearing any clothes? Can J Cardiol 2017;33(6):747-57.
8. Choi Y, Kim SM, Lee SC, Chang SA, Jang SY, Choe YH. Quantification of left ventricular trabeculae using cardiovascular magnetic resonance for the diagnosis of left ventricular non-compaction: evaluation of trabecular volume and refined semi-quantitative criteria. J Cardiovasc Magn Reson 2016;18(1):24.
9. Grothoff M, Pachowsky M, Hoffmann J, Posch M, Klaassen S, Lehmkuhl L, Gutberlet M. Value of cardiovascular MR in diagnosing left ventricular non-compaction cardiomyopathy and in discriminating between other cardiomyopathies. Eur Radiol 2012;22(12):2699-709.
10. Ivanov A, Dabiesingh DS, Bhumireddy GP, Mohamed A, Asfour A, Briggs WM, et al. Prevalence and prognostic significance of left ventricular noncompaction in patients referred for cardiac magnetic resonance imaging. Circ Cardiovasc Imaging 2017;10(9):e006174.
11. Jacquier A, Thuny F, Jop B, Giorgi R, Cohen F, Gaubert JY, et al. Measurement of trabeculated left ventricular mass using cardiac magnetic resonance imaging in the diagnosis of left ventricular non-compaction. Eur Heart J 2010;31(9):1098-104.
12. Kini V, Ferrari VA, Han Y, Jha S. Adherence to thresholds: overdiagnosis of left ventricular noncompaction cardiomyopathy. Acad Radiol 2015;22(8):1016-9.
13. Niemann M, Stork S, Weidemann F. Left ventricular noncompaction cardiomyopathy: an overdiagnosed disease. Circulation 2012;126(16):e240-3.
14. Paterick TE, Tajik AJ. Left ventricular noncompaction: a diagnostically challenging cardiomyopathy. Circ J 2012;76(7):1556-62.
15. Petersen SE, Selvanayagam JB, Wiesmann F, Robson MD, Francis JM, Anderson RH, et al. Left ventricular non-compaction: insights from cardiovascular magnetic resonance imaging. J Am Coll Cardiol 2005;46(1):101-5.
16. Stollberger C, Finsterer J. Pitfalls in the diagnosis of left ventricular hypertrabeculation/non-compaction. Postgrad Med J 2006;82(972):679-83.
17. Weir-McCall JR, Yeap PM, Papagiorcopulo C, Fitzgerald K, Gandy SJ, Lambert M, et al. Left ventricular noncompaction: anatomical phenotype or distinct cardiomyopathy? J Am Coll Cardiol 2016;68(20):2157-65.
18. Jenni R, Oechslin E, Schneider J, Attenhofer Jost C, Kaufmann PA. Echocardiographic and pathoanatomical characteristics of isolated left ventricular non-compaction: a step towards classification as a distinct cardiomyopathy. Heart 2001;86(6):666-71.
19. Schulz-Menger J, Bluemke DA, Bremerich J, Flamm SD, Fogel MA, Friedrich MG, et al. Standardized image interpretation and post processing in cardiovascular magnetic resonance: Society for Cardiovascular Magnetic Resonance (SCMR) Board of Trustees Task Force on Standardized Post Processing. J Cardiovasc Magn Reson 2013;15:35.

20. Jefferies JL, Wilkinson JD, Sleeper LA, Colan SD, Lu M, Pahl E, et al. Cardiomyopathy phenotypes and outcomes for children with left ventricular myocardial noncompaction: results from the Pediatric Cardiomyopathy Registry. J Card Fail 2015;21(11):877-84.
21. Braunwald E. Cardiomyopathies: an overview. Circ Res 2017;121(7):711-21.
22. Arbustini E, Favalli V, Narula N, Serio A, Grasso M. Left ventricular noncompaction: a distinct genetic cardiomyopathy? J Am Coll Cardiol 2016;68(9):949-66.
23. Brescia ST, Rossano JW, Pignatelli R, Jefferies JL, Price JF, Decker JA, et al. Mortality and sudden death in pediatric left ventricular noncompaction in a tertiary referral center. Circulation 2013;127(22):2202-8.
24. D'Amato G, Luxan G, del Monte-Nieto G, Martinez-Poveda B, Torroja C, Walter W, et al. Sequential Notch activation regulates ventricular chamber development. Nat Cell Biol 2016;18(1):7-20.
25. Garcia-Pavia P, de la Pompa JL. Left ventricular noncompaction: a genetic cardiomyopathy looking for diagnostic criteria [published erratum appears in J Am Coll Cardiol 2015;65(5):519]. J Am Coll Cardiol 2014;64(19):1981-3.
26. Jensen B, van der Wal AC, Moorman AFM, Christoffels VM. Excessive trabeculations in noncompaction do not have the embryonic identity. Int J Cardiol 2017;227:325-30.
27. Miszalski-Jamka K, Jefferies JL, Mazur W, Glowacki J, Hu J, Lazar M, et al. Novel genetic triggers and genotype-phenotype correlations in patients with left ventricular noncompaction. Circ Cardiovasc Genet 2017;10(4):e001763.
28. Morcos PN, Andersson UME, Adler ED. Left ventricular non-compaction: current controversy and new insights. J Genet Syndr Gene Ther 2015;6(1). doi:10.4172/2157-7412.1000255.
29. Oechslin E, Jenni R. Left ventricular non-compaction revisited: a distinct phenotype with genetic heterogeneity? Eur Heart J 2011;32(12):1446-56.
30. Quarta G, Papadakis M, Donna PD, Maurizi N, Iacovoni A, Gavazzi A, et al. Grey zones in cardiomyopathies: defining boundaries between genetic and iatrogenic disease. Nat Rev Cardiol 2017;14(2):102-12.
31. Samsa LA, Yang B, Liu J. Embryonic cardiac chamber maturation: trabeculation, conduction, and cardiomyocyte proliferation. Am J Med Genet C Semin Med Genet 2013;163C(3):157-68.
32. Sasse-Klaassen S, Probst S, Gerull B, Oechslin E, Nurnberg P, Heuser A, et al. Novel gene locus for autosomal dominant left ventricular noncompaction maps to chromosome 11p15. Circulation 2004;109(22):2720-3.
33. Towbin JA, Jefferies JL. Cardiomyopathies due to left ventricular noncompaction, mitochondrial and storage diseases, and inborn errors of metabolism. Circ Res 2017;121(7):838-54.
34. Zhang W, Chen H, Qu X, Chang CP, Shou W. Molecular mechanism of ventricular trabeculation/compaction and the pathogenesis of the left ventricular noncompaction cardiomyopathy (LVNC). Am J Med Genet C Semin Med Genet 2013;163C(3):144-56.
35. Landrum MJ, Lee JM, Benson M, Brown G, Chao C, Chitipiralla S, et al. ClinVar: public archive of interpretations of clinically relevant variants. Nucleic Acids Res 2016;44(D1):D862-8.
36. Richard P, Ader F, Roux M, Donal E, Eicher JC, Aoutil N, et al. Targeted panel sequencing in adult patients with left ventricular non-compaction reveals a large genetic heterogeneity. Clin Genet 2019;95(3):356-67.
37. Bennett CE, Freudenberger R. The current approach to diagnosis and management of left ventricular noncompaction cardiomyopathy: review of the literature. Cardiol Res Pract 2016;2016:5172308.
38. Lee TM, Hsu DT, Kantor P, Towbin JA, Ware SM, Colan SD, et al. Pediatric cardiomyopathies. Circ Res 2017;121(7):855-73.
39. Lipshultz SE, Cochran TR, Briston DA, Brown SR, Sambatakos PJ, Miller TL, et al. Pediatric cardiomyopathies: causes, epidemiology, clinical course, preventive strategies and therapies. Future Cardiol 2013;9(6):817-48.
40. Pulignano G, Tinti MD, Tolone S, Musto C, De Lio L, Pino PG, et al. Noncompaction and embolic myocardial infarction: the importance of oral anticoagulation. Rev Port Cardiol 2015;34(7-8):497.e1-4.
41. Pignatelli RH, McMahon CJ, Dreyer WJ, Denfield SW, Price J, Belmont JW, et al. Clinical characterization of left ventricular noncompaction in children: a relatively common form of cardiomyopathy. Circulation 2003;108(21):2672-8.
42. Weisz SH, Limongelli G, Pacileo G, Calabro P, Russo MG, Calabro R, Vatta M. Left ventricular non compaction in children. Congenit Heart Dis 2010;5(5):384-97.
43. Greutmann M, Mah ML, Silversides CK, Klaassen S, Attenhofer Jost CH, Jenni R, Oechslin EN. Predictors of adverse outcome in adolescents and adults with isolated left ventricular noncompaction. Am J Cardiol 2012;109(2):276-81.
44. Thavendiranathan P, Dahiya A, Phelan D, Desai MY, Tang WH. Isolated left ventricular non-compaction controversies in diagnostic criteria, adverse outcomes and management. Heart 2013;99(10):681-9.
45. Aryal MR, Badal M, Giri S, Pradhan R. Left ventricular non-compaction presenting with heart failure and intramural thrombus. BMJ Case Rep 2013;2013:bcr2013009757.
46. Blinder JJ, Martinez HR, Craigen WJ, Belmont J, Pignatelli RH, Jefferies JL. Noncompaction of the left ventricular myocardium in a boy with a novel chromosome 8p23.1 deletion. Am J Med Genet A 2011;155A(9):2215-20.
47. Cohen PJ, Prahlow JA. Sudden death due to biventricular non-compaction cardiomyopathy in a 14-year-old. Forensic Sci Med Pathol 2015;11(1):92-8.
48. de Melo MD, Benvenuti LA, Mady C, Kalil-Filho R, Salemi VM. Left ventricular basal region involvement in noncompaction cardiomyopathy. Cardiovasc Pathol 2013;22(6):503-4.
49. Jacobs K, Giacobbe L, Aguilera M, Ramin K, Sivanandam S. A case of fetal diagnosis of noncompaction cardiomyopathy and coarctation of the aorta. AJP Rep 2014;4(1):45-8.
50. Oechslin EN, Attenhofer Jost CH, Rojas JR, Kaufmann PA, Jenni R. Long-term follow-up of 34 adults with isolated left ventricular noncompaction: a distinct cardiomyopathy with poor prognosis. J Am Coll Cardiol 2000;36(2):493-500.
51. Peters F, Dos Santos C, Essop R. Isolated left ventricular non-compaction with normal ejection fraction. Cardiovasc J Afr 2011;22(2):90-3.
52. Ridha A, Khan A, Al-Abayechi S, Yeung E. Clinical dilemma: recurrent syncope with isolated left ventricle non-compaction cardiomyopathy and preserved ejection fraction, a case report and review of the literature. J Med Cases 2015;6(2):77-80.
53. Ridha M, Batra S, Collins J, Montgomery J, Ho D, Voetsch B. Left ventricular non-compaction: a rare cause of stroke in the young. Neurology 2018;90(15 Suppl):p6.232.
54. Khanna RR, Garg R, Madan H, Mahajan N, Kumar P. Isolated ventricular non-compaction syndrome, rare cause of recurrent stroke in young - a case report. J Neurol Neurosci 2016;7(3):99.

55. Vinograd CA, Srivastava S, Panesar LE. Fetal diagnosis of left-ventricular noncompaction cardiomyopathy in identical twins with discordant congenital heart disease. Pediatr Cardiol 2013;34(6):1503-7.
56. Wald R, Veldtman G, Golding F, Kirsh J, McCrindle B, Benson L. Determinants of outcome in isolated ventricular noncompaction in childhood. Am J Cardiol 2004;94(12):1581-4.
57. Wats K, Chen O, Uppal NN, Batul SA, Moskovits N, Shetty V, Shani J. A rare case of renal infarct due to noncompaction cardiomyopathy: a case report and literature review. Case Rep Cardiol 2016;2016:6789149.
58. Kawel N, Nacif M, Arai AE, Gomes AS, Hundley WG, Johnson WC, et al. Trabeculated (noncompacted) and compact myocardium in adults: the multi-ethnic study of atherosclerosis. Circ Cardiovasc Imaging 2012;5(3):357-66.
59. Shi WY, Moreno-Betancur M, Nugent AW, Cheung M, Colan S, Turner C, et al. Long-term outcomes of childhood left ventricular noncompaction cardiomyopathy: results from a national population-based study. Circulation 2018;138(4):367-76.
60. Caselli S, Ferreira D, Kanawati E, Di Paolo F, Pisicchio C, Attenhofer Jost C, et al. Prominent left ventricular trabeculations in competitive athletes: a proposal for risk stratification and management. Int J Cardiol 2016; 223:590-5.
61. Gati S, Sharma S. CardioPulse: the dilemmas in diagnosing left ventricular non-compaction in athletes. Eur Heart J 2015;36(15):891-3.
62. Suinesiaputra A, Bluemke DA, Cowan BR, Friedrich MG, Kramer CM, Kwong R, et al. Quantification of LV function and mass by cardiovascular magnetic resonance: multi-center variability and consensus contours. J Cardiovasc Magn Reson 2015;17:63.
63. Moody WE, Edwards NC, Chue CD, Taylor RJ, Ferro CJ, Townend JN, Steeds RP. Variability in cardiac MR measurement of left ventricular ejection fraction, volumes and mass in healthy adults: defining a significant change at 1 year. Br J Radiol 2015;88(1049):20140831.
64. Chuang ML, Gona P, Hautvast GL, Salton CJ, Breeuwer M, O'Donnell CJ, Manning WJ. CMR reference values for left ventricular volumes, mass, and ejection fraction using computer-aided analysis: the Framingham Heart Study. J Magn Reson Imaging 2014;39(4):895-900.
65. Corsi C, Veronesi F, Lamberti C, Bardo DM, Jamison EB, Lang RM, Mor-Avi V. Automated frame-by-frame endocardial border detection from cardiac magnetic resonance images for quantitative assessment of left ventricular function: validation and clinical feasibility. J Magn Reson Imaging 2009;29(3):560-8.
66. Marino M, Veronesi F, Corsi C. Fully automated assessment of left ventricular volumes and mass from cardiac magnetic resonance images. Conf Proc IEEE Eng Med Biol Soc 2014;2014:1079-82.
67. Marino M, Corsi C, Maffessanti F, Patel AR, Mor-Avi V. Objective selection of short-axis slices for automated quantification of left ventricular size and function by cardiovascular magnetic resonance. Clin Imaging 2016;40(4):617-23.
68. Caiani EG, Colombo A, Pepi M, Piazzese C, Maffessanti F, Lang RM, Carminati MC. Three-dimensional left ventricular segmentation from magnetic resonance imaging for patient-specific modelling purposes. Europace 2014;16 Suppl 4:iv96-iv101.
69. Wang L, Pei M, Codella NC, Kochar M, Weinsaft JW, Li J, et al. Left ventricle: fully automated segmentation based on spatiotemporal continuity and myocardium information in cine cardiac magnetic resonance imaging (LV-FAST). Biomed Res Int 2015;2015:367583.
70. Bai W, Sinclair M, Tarroni G, Oktay O, Rajchl M, Vaillant G, et al. Automated cardiovascular magnetic resonance image analysis with fully convolutional networks. J Cardiovasc Magn Reson 2018;20(1):65.
71. Cai J, Bryant JA, Le TT, Su B, de Marvao A, O'Regan DP, et al. Fractal analysis of left ventricular trabeculations is associated with impaired myocardial deformation in healthy Chinese. J Cardiovasc Magn Reson 2017;19(1):102.